

# Evidence for trimers evaporation in silver bromide clusters

J.-M. L'Hermite<sup>1,a</sup>, F. Rabilloud<sup>1</sup>, P. Labastie<sup>1</sup>, and F. Spiegelman<sup>2</sup><sup>1</sup> Laboratoire CAR/IRSAMC<sup>b</sup>, Université Paul Sabatier, 118 route de Narbonne, F-30062 Toulouse Cedex, France<sup>2</sup> LPQ/IRSAMC<sup>c</sup>, Université Paul Sabatier, 118 route de Narbonne, F-30062 Toulouse Cedex, France

Received 28 November 2000

**Abstract.** Metastable fragmentation channels of free silver bromide clusters  $(\text{Ag}_n\text{Br}_p)^+$  are reported. The large majority release a neutral trimer  $(\text{AgBr})_3$ . This is interpreted in the frame of *ab initio* DFT calculations with 19-electron pseudopotential on silver atom. The stability, the structural and electronic properties of  $(\text{Ag}_n\text{Br}_p)^{(\pm)}$  ( $n = 6, p = n, n - 1$ ) are examined. The structures of the clusters are different from expected in electrostatic models. The 3D transition has not yet happened: the calculated ground state structures of  $(\text{AgBr})_n \leq 6$  clusters are quasi two-dimensional. Our work rationalizes the part of covalence in the Ag-Br interaction and the role of *d* electrons of silver. The known abundance of trimers in the vapor of silver bromide, but also of other silver and cuprous halides is for the first time explained as an indirect consequence of the covalent interaction between metal ions.

**PACS.** 36.40.Qv Stability and fragmentation of clusters – 31.15.Ar Ab initio calculations

## 1 Introduction

The trimer is known to play a special role in noble metal halides in the gas phase: an amazing common property of all these compounds is the unusual abundance of trimers in their vapor [1–5]. The vapor of cuprous halides CuCl, CuBr, CuI contains mainly trimers but also tetramers [1–4], whereas monomers and dimers are roughly equally abundant in the vapors of AgCl, AgBr and AgI [5]. It has also been demonstrated that the trimer is a building block in silver hydroxide clusters [6–8]. Another common point is the ionic-covalent nature of bonding in both cuprous and silver halides. The copper halides are often considered as “covalent with a slightly ionic character” whereas silver halides are described as “ionic with a slightly covalent character” [9]. It is obviously due to their isoelectronic shells ( $\dots 3d^{10}4s^1$  for copper,  $\dots 4d^{10}5s^1$  for silver). Some properties of silver halides in the bulk phase have been attributed to covalence as far back as 1960. Jansen and coworkers [10] mentioned that the pressure transition of AgBr, AgF and AgCl from the NaCl to the CsCl structure cannot be explained in the framework of an ionic pair potential model, and showed that Many-Body interactions must be taken into account, suggesting covalent interactions. Fischer [11] and Dorner [12] explained the anomalous phonon dispersion curves of silver halides observed by Raman spectroscopy by covalent coupling of  $\text{Ag}^+$  ions to their neighbors. In this paper, we shall clarify the assumption of a “partial covalence” in silver bromide com-

pounds through an experimental and theoretical study of silver bromide clusters. We shall show that the particular status of the trimer mentioned above is actually an indirect consequence of this partial covalence, and we shall see that the structures of quasi stoichiometric clusters are quite different from the ones expected from electrostatic models. We shall also discuss the extension of our interpretations to other previously misunderstood experiments on silver and cuprous halides.

## 2 Experiment

The experimental setup has already been detailed elsewhere [13]. The source is based on laser vaporization of a silver bromide rotating rod using a 532 nm Nd:YAG laser. Clusters are seeded in helium gas and mass selected in a Reflectron-Time-Of-Flight (RETOF) mass spectrometer. We developed a new method for analyzing the metastable fragmentation which occurs in the free field region [14]. Briefly, it consists in scanning the voltage of the end plate of the reflectron, and then plot the evolution of the time of flight peaks as a function of the inverse of this voltage. The points are aligned on straight lines. Each straight line corresponds to a given (parent, fragment) couple. The intersection with the *Y*-axis corresponds to a infinite repulsive voltage: in this case, the cluster spends no time in the reflectron. Knowing that the time of flight spent out of the reflectron depends only on the mass of the parent, this quantity can unambiguously be deduced from the intersection time. It is also easy to show that the slope of the straight line is proportional to the mass of the

---

<sup>a</sup> e-mail: j-m.lhermite@irsamc.ups-tlse.fr<sup>b</sup> CNRS UMR 5589<sup>c</sup> CNRS UMR 5626

fragment. The fragmentation of  $\text{Ag}_n\text{Br}_{n-1}^+$  clusters have been studied using this novel method.

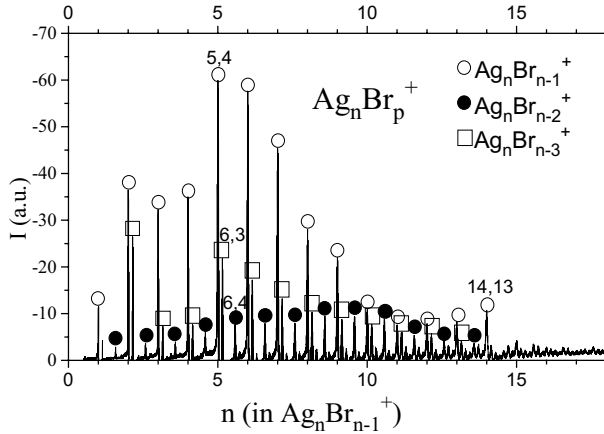


**Fig. 1.** Mass spectrum of positively charged silver bromide clusters.

### 3 Theory

*Ab initio* calculations have been performed in the framework of the Density Functional Theory (DFT) using the B3LYP functional [15]. Both Ag and Br atoms were represented through relativistic effective core pseudopotential. Silver was considered an  $[\text{Ag}^{19+}]$  core with  $4s$ ,  $4p$ ,  $4d$  and  $5s$  active electrons. Bromine was described as a  $[\text{Br}^{7+}]$  core with  $4s$  and  $4p$  active electrons. The Gaussian basis set was  $8s7p6d$  contracted into  $6s5p3d$  on silver. The influence of an extra  $f$  function was examined. A  $5s6p1d$  basis contracted into  $3s3p1d$  was used on bromine. The validity of this treatment has been checked by comparing the results for the smallest clusters  $(\text{Ag}_n\text{Br}_p)^{+}$  ( $n, p \leq 2$ ) to those obtained in a more accurate configuration interaction approach [16]. The ground state structures of  $(\text{Ag}_n\text{Br}_p)^{+}$  ( $n \leq 6, p = n, n-1$ ) have been calculated. The optimization process was carried out using gradient algorithms starting with sets of guessed isomer structures predetermined with empirical models and taken from known structures for other ionic systems [8,17].

### 4 Results and discussion

A typical mass spectrum of positively charged silver bromide clusters recorded under normal RETOF operation mode is shown in Figure 1. The main observed series corresponds to stoichiometric  $\text{Ag}_n\text{Br}_{n-1}^+$  clusters. Two other characteristic features already seen in previous experiments [18] can be noticed: first, as in the case of alkali halide clusters,  $\text{Ag}_{14}\text{Br}_{13}^+$  appears with a large abundance, revealing probably a  $3 \times 3 \times 3$  cubic structure known to

be very stable in ionic systems. Second,  $\text{Ag}_5\text{Br}_4^+$  also appears with a large intensity. This is not expected in an ionic scheme; as we shall see in the next section, it is due to the particular fragmentation patterns of silver bromide clusters. It is not possible to extract much more information from the mass spectra since the relative abundance strongly depends on the source parameters (carrier gas pressure, vaporization laser fluence, opening duration of the pulsed valve, various delays, ...). A more powerful investigation tool is the analysis of the metastable fragmentation channels that we shall present in the next paragraph.

#### 4.1 Fragmentation patterns

The so-called metastable fragmentation is the spontaneous evaporation that undergo clusters whose internal energy is larger than their dissociation energy. It occurs on time scales much larger than the characteristic vibrational periods (a few picoseconds). In our experiment, the observation time window is of the order of microseconds. A rigorous interpretation of the evaporation rates should take into account not only the dissociation energies, but also the variation of entropy in the fragmentation process (in particular when large fragments are released as in our case) and eventual potential barriers along the fragmentation path. Unfortunately, there are no statistical decay models to our knowledge which deals correctly with entropy [19,20]. By chance, these entropy effects are not expected to introduce importance changes in the fragmentation patterns, but only to modify the exact values of the branching ratios. Concerning the potential barriers, we have some reasons to believe that they are not important in our systems [21]. So the fragmentation ratio will be interpreted in the following as depending only on the dissociation energy.

A typical fragmentation spectrum is shown in Figure 2. Clusters were not warmed up downstream from the source, but we only slightly increased the fluence of the vaporization laser, producing in this way hot clusters which spontaneously dissociated in the free field region of the mass spectrometer. Each peak in Figure 2 corresponds to a given (parent, fragment) fragmentation channel shown in Table 1. All the major peaks result from the fragmentation of  $\text{Ag}_n\text{Br}_{n-1}^+$  clusters. Very strikingly the most frequently observed decay channel is  $\text{Ag}_n\text{Br}_{n-1}^+ \rightarrow \text{Ag}_{n-3}\text{Br}_{n-4}^+ + (\text{AgBr})_3$ .  $\text{Ag}_6\text{Br}_5^+$  is an exception and evaporates preferentially  $\text{AgBr}$ . Nevertheless, the fragmentation into  $(\text{AgBr})_3$  also occurs since its dissociation energy is very close (+0.02 eV). Non stoichiometric clusters  $\text{Ag}_n\text{Br}_{n-2,3,5}^+$  follow the same scheme and evaporate also preferentially  $(\text{AgBr})_3$ . Fragmentation rates and branching ratios have been determined by comparing the signal recorded in fragmentation experiments and under the normal RETOF operation mode. The fragmentation rates, of the order of a few percent for  $n \leq 6$ , sharply increases from  $n = 7$  to reach about 13% at  $n = 10$ . The low dissociation rate of  $\text{Ag}_6\text{Br}_5^+$  into  $(\text{AgBr})_3$  is easy to understand since there are two quasi-degenerate channels with a

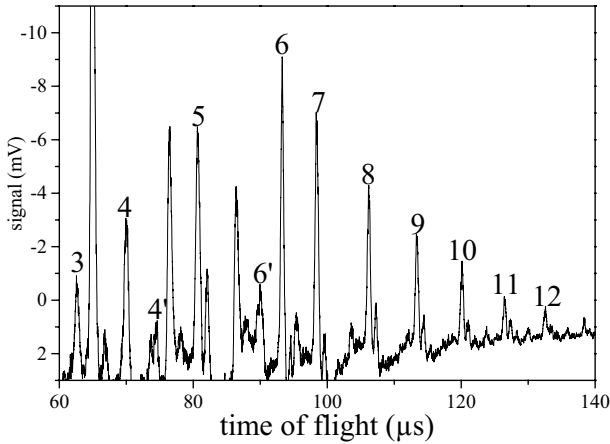


**Fig. 2.** Fragmentation spectrum of silver bromide clusters. The reaction corresponding to each peak is detailed in table 1. The large majority of the most intense peaks (4, 5, 6', 7, 8, 9, 10, 11, 12) correspond to the evaporation of  $(\text{AgBr})_3$ .

**Table 1.** Lowest fragmentation channels for  $\text{Ag}_n\text{Br}_{n-1}^+$ . The couples  $n, p$  refer to the number of silver and bromine atoms in  $\text{Ag}_n\text{Br}_p$ . The last column is the numbering of figure 2.  $D_n$  are the calculated dissociation energies from ref. [5]. \* The ground state energy of  $\text{Ag}_6\text{Br}_5^+$  is unknown. Nevertheless, it is possible to calculate the dissociation energies to a constant  $\Delta$ .

parent	fragments	rate (%)	$D_n$ (eV)	$n^\circ$
2, 1 <sup>+</sup>	1, 0 <sup>+</sup> + 1, 1	0.15	2.09	
3, 2 <sup>+</sup>	2, 1 <sup>+</sup> + 1, 1	1.9	1.64	3
4, 3 <sup>+</sup>	1, 0 <sup>+</sup> + <b>3, 3</b>	1.2	1.66	4
	3, 2 <sup>+</sup> + 1, 1	1.5	1.78	4'
5, 4 <sup>+</sup>	2, 1 <sup>+</sup> + <b>3, 3</b>	1.2	1.66	5
6, 5 <sup>+</sup>	5, 4 <sup>+</sup> + 1, 1	6.3	$\Delta$ *	6
	3, 2 <sup>+</sup> + <b>3, 3</b>	1.2	$\Delta + 0.02$ *	6'
7, 6 <sup>+</sup>	4, 3 <sup>+</sup> + <b>3, 3</b>	5.8		7
8, 7 <sup>+</sup>	5, 4 <sup>+</sup> + <b>3, 3</b>	9.8		8
9, 8 <sup>+</sup>	6, 5 <sup>+</sup> + <b>3, 3</b>	11.5		9
10, 9 <sup>+</sup>	7, 6 <sup>+</sup> + <b>3, 3</b>	12.8		10
11, 10 <sup>+</sup>	8, 7 <sup>+</sup> + <b>3, 3</b>	12.0		11

higher probability for the release of a molecular monomer  $\text{AgBr}$ . The large abundance of  $\text{Ag}_5\text{Br}_4^+$  in the mass spectra recorded under normal conditions [21] is also easily understood if one considers that the observed clusters come from the dissociation of larger ones, according to the hypothesis of the evaporative ensemble of Klotz which states that any observed cluster comes from at least one dissociation [22]: under this assumption,  $\text{Ag}_5\text{Br}_4^+$  come from two dissociation channels: a)  $\text{Ag}_6\text{Br}_5^+ \rightarrow \text{Ag}_5\text{Br}_4^+ + \text{AgBr}$  and b)  $\text{Ag}_8\text{Br}_7^+ \rightarrow \text{Ag}_5\text{Br}_4^+ + (\text{AgBr})_3$ . The large abundance of  $\text{Ag}_5\text{Br}_4^+$  is an indirect proof of the particular dissociation channel for  $\text{Ag}_6\text{Br}_5^+$ .

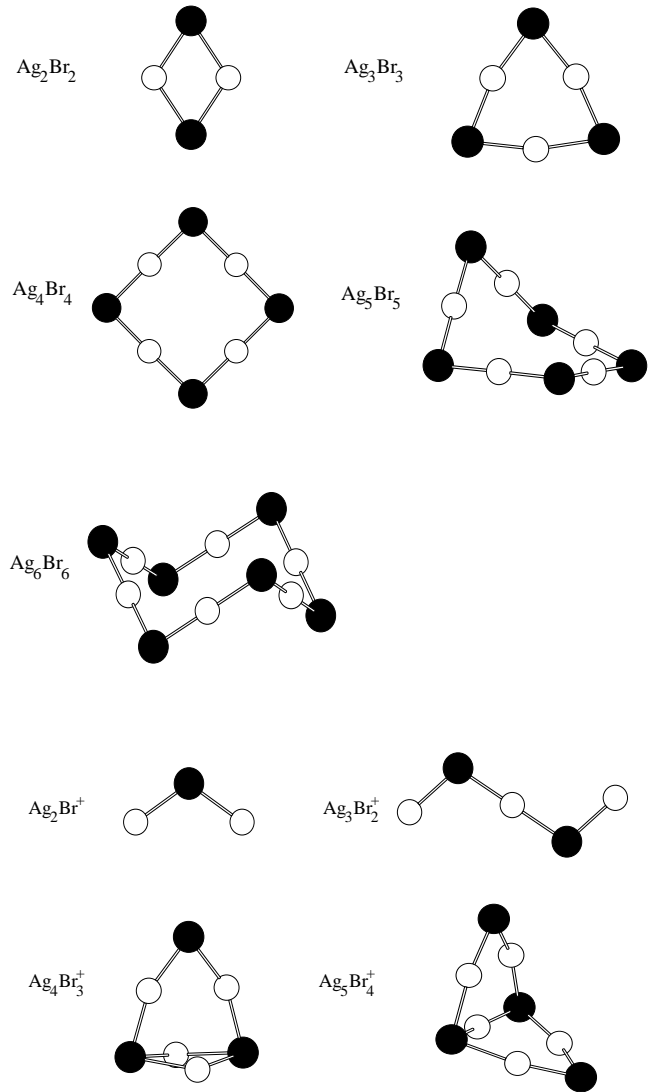


**Fig. 3.** The ground state structure of neutral  $(\text{AgBr})_n$  and cationic  $\text{Ag}_n\text{Br}_{n-1}^+$  clusters.

## 4.2 Calculated structures

The calculated ground state structures of  $\text{Ag}_n\text{Br}_{n-1}^+$  and  $\text{Ag}_n\text{Br}_n$  are shown in Figure 3. Let us first point out that these calculations are validated by the excellent agreement of the calculated dissociation channels with the experimental data (see Table 1). All the lowest isomers ( $n \leq 6$ ) are planar or nonplanar cycles.  $(\text{AgBr})_2$  and  $(\text{AgBr})_3$  are respectively rhomboedric and quasi triangular with bromines at the apexes. These structures are frequently encountered for ionic clusters. More surprising are the structures of larger clusters. The ground state of  $(\text{AgBr})_4$  is a square bent around a Br-Br diagonal. The expected cublike structure (slightly distorted) is also stable but lies 1.07 eV above the ground state.  $(\text{AgBr})_5$  remains cyclic, it is a distorted pentagon. The hexamer is also a cycle distorted around Br-Br axis. The shape of  $(\text{Ag}_n\text{Br}_{n-1})^+$  clusters also differ from the ones of “standard” ionic clusters.  $\text{Ag}_3\text{Br}_2^+$  is a chain with bent Ag-Br-Ag substructures.

$\text{Ag}_4\text{Br}_3^+$  looks like  $(\text{AgBr})_3$  with two instead of one silver atoms on one edge.  $\text{Ag}_5\text{Br}_4^+$  is made of two  $(\text{AgBr})_3$  subunits sharing an edge.

All these structures result, in addition to the Coulomb forces, from the following interactions: first, the high polarizability of bromide ion which favors the structures maximizing the electric field on the bromide ions, second the three-body interactions due to the mixing of  $4d$  orbitals of silver and  $4p$  orbitals of bromine illustrated on Figure 4 in the case of  $(\text{AgBr})_3$ . These two types of interaction favor the formation of  $\text{BrAgBr}$  linear subunits and tend to bend the  $\text{AgBrAg}$  subunits (in all clusters the  $\widehat{\text{AgBrAg}}$  angles are about 110 degrees). An electrostatic model including Coulomb plus polarization forces added to Born-Mayer repulsive contributions does not reproduce the structures obtained in the *ab initio* calculations. This confirms the partial covalent character of the Ag-Br bonding. One can notice that a simple potential model which accounts empirically for the geometrical constraints on the  $\text{BrAgBr}$  and  $\text{AgBrAg}$  triatomic subunits has been able to generate the same ground state structures as those obtained in *ab initio* calculations for  $(\text{AgBr})_{n=2\dots 5}$  and  $(\text{Ag}_{n=2\dots 5}\text{Br}_{n-1})^+$ . To summarize, the  $d$  orbitals of silver atoms are for a large part responsible for the specificity of silver bromide clusters.

Let us mention finally that the release of  $(\text{AgBr})_3$  trimer is also the lowest calculated dissociation channel for stoichiometric clusters  $(\text{AgBr})_{n=4\dots 6}$ .

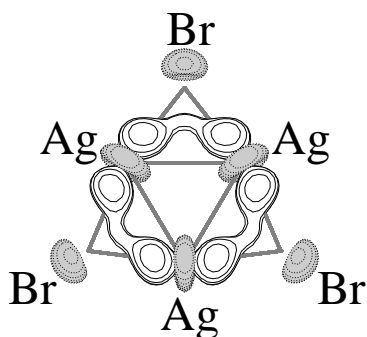


**Fig. 4.** Contour plot of a binding molecular orbital of  $(\text{AgBr})_3$  made of a mixing of  $4d$  orbitals of Ag and  $4p$  orbitals of Br.

## 5 Conclusion

The evaporation of a trimer has been experimentally demonstrated to be the preferred dissociation channel of silver bromide clusters. It seems that the effect of  $d$  orbitals should not be restricted to silver bromide and may be

extended to other monovalent compounds of silver, and even to cuprous halides (the electronic structure of copper is  $\dots 3d^{10}4s^1$ ): Bertolus and coworkers obtained very similar structures for  $\text{Ag}_{n \leq 4}\text{OH}_{n,n-1}^{(+)}$  [8], and the vibrational spectra of matrix isolated  $(\text{Cu-halide})_{n=4\dots 8}$  clusters was interpreted by Martin as resulting from quasipolar structures [3, 4]. Moreover, if one considers the peculiar stability of the trimer  $(\text{AgBr})_3$  as a kind of signature of the effect of  $d$  orbitals, the abundance of the trimer in the vapors of silver and cuprous halides is readily understood.

## References

1. M. Binnewies, K. Rinke, H. Schäfer, Z. Anorg. Chem. **395**, 51 (1972).
2. M. Binnewies, H. Schäfer, Z. Anorg. Chem. **395**, 63 (1972).
3. T.P. Martin, H. Shaber, J. Chem. Phys. **73**, 3541 (1980).
4. T.P. Martin, A. Kakizaki, J. Chem. Phys. **80**, 3956 (1984).
5. J. Berkowitz, C.H. Batson, G.L. Goodman, J. Chem. Phys. **72**, 5829 (1980).
6. C. Bréchnignac, Ph. Cahuzac, J. Leygnier, I. Tignères, Eur. Phys. J. D **9**, 421 (1999).
7. C. Bréchnignac, Ph. Cahuzac, J. Leygnier, I. Tignères, Chem. Phys. Lett. **303**, 304 (1999).
8. M. Bertolus, V. Brenner, P. Millié, Eur. Phys. J. D **11**, 387 (2000).
9. F.C Brown, *The Physics of Solid* (W.A. Benjamin, Inc, New-York, 1967).
10. L. Jansen, E. Lombardi, Phys. Rev. Lett. **12**, 11 (1964).
11. K. Fischer, H. Biz, R. Haberkorn, W. Weber, Phys. Stat. Sol. (b) **54**, 285 (1972).
12. B. Dorner, W. von der Osten, W. Bühner, J. Phys. C: Solid State Phys. **9**, 723 (1976).
13. P. Labastie, J.-M. L'Hermite, P. Poncharal, M. Sence, J. Chem. Phys. **103**, 6362 (1995).
14. J.-M. L'Hermite, L. Marcou, F. Rabilloud, P. Labastie, Rev. Sci. Ins. **71**, 2033 (2000).
15. F. Rabilloud, F. Spiegelmann, J.-M. L'Hermite, P. Labastie, J. Chem. Phys. **114**, 289 (2001).
16. F. Rabilloud, F. Spiegelmann, J.-L. Heully, J. Chem. Phys. **111**, 8925 (1999).
17. G. Durand, J. Giraud-Girard, D. Maynau, F. Spiegelmann, F. Calvo, J. Chem. Phys. **110**, 7871 (1999).
18. I. Rabin, C. Jackschatz, W. Shulze, F.W. Froben, Z. Phys. D **19**, 401 (1991).
19. C. Bréchnignac, Ph. Cahuzac, M. De Frutos, A. Sarfati, V. Akulin, Phys. Rev. Lett. **77**, 251 (1996).
20. C. Bréchnignac, Ph. Cahuzac, N. Kébaïli, J. Leygnier, J. Chem. Phys. **112**, 10197 (2000).
21. J.-M. L'Hermite, F. Rabilloud, L. Marcou, P. Labastie, Eur. Phys. J. D **14**, 323 (2001).
22. C.E. Klotz, J. Chem. Phys. **83**, 5854 (1985).